Temperature dependence and magnetocrystalline anisotropy studies of self-assembled L 1 0 -Fe 55 Pt 45 ferromagnetic nanocrystals

L. C. Varanda, M. Jafelicci Jr., and M. Imaizumi

Citation: Journal of Applied Physics **101**, 123918 (2007); doi: 10.1063/1.2747209
View online: http://dx.doi.org/10.1063/1.2747209
View Table of Contents: http://scitation.aip.org/content/aip/journal/jap/101/12?ver=pdfcov
Published by the AIP Publishing

Temperature dependence and magnetocrystalline anisotropy studies of self-assembled $L1_0$-$Fe_{55}Pt_{45}$ ferromagnetic nanocrystals

L. C. Varanda[a] and M. Jafelicci, Jr.
Institute of Chemistry - UNESP, Laboratory of Magnetic Materials and Colloids, Department of Physical-Chemistry, P.O. Box 355, 14801-970 Araraquara, SP, Brazil

M. Imaizumi
Faculty of Science - UNESP, Department of Physics, Av. Luiz Edmundo Carrijo Coube S/N, 17033-360 Bauru, Brazil

(Received 10 January 2007; accepted 28 April 2007; published online 26 June 2007)

Temperature dependence and uniaxial magnetocrystalline anisotropy properties of the chemically synthesized 4 nm $L1_0$-$Fe_{55}Pt_{45}$ nanoparticle assembly by a modified polyol route are reported. As-prepared nanoparticles are superparamagnetic presenting fcc structure, and annealing at 550 °C converts the assembly into ferromagnetic nanocrystals with large coercivity ($H_C > 1$ T) in an $L1_0$ phase. Magnetic measurements showed an increasing in the ferromagnetically ordered fraction of the nanoparticles with the annealing temperature increases, and the remanence ratio, $S = M_R/M_S \cong 0.76$, suggests an (111) textured film. A monotonic increase of the blocking temperature T_B, the uniaxial magnetocrystalline anisotropy constant K_U, and the coercivity H_C with increasing annealing temperature was observed. Magnetic parameters indicate an enhancement in the magnetic properties due to the improved $Fe_{55}Pt_{45}$ phase stabilizing, and the room-temperature stability parameter of 67, which indicates that the magnetization should be stable for more than ten years, makes this material suitable for ultrahigh-density magnetic recording application. © *2007 American Institute of Physics*. [DOI: 10.1063/1.2747209]

I. INTRODUCTION

The areal density in magnetic recording has reached 20 Gbit/in.^{2} in products and has been increasing at a rate of ~130% per year since 1997. Data rates are approaching Gbit/s levels and are increasing at a rate of ~40% per year.[1] An area of particular importance is media noise suppression, which involves the reduction and scaling of the media grain size, control of the magnetic grain isolation, and uniformity and control of the crystallographic texturing. The resultant dramatic reduction of the bit size has led to the rapid scaling of the characteristic grain size and to the corresponding shrinkage of the thermal activation volume in conventional polycrystalline media. This, in turn, has led to challenging issues related to long-term data stability.[2] Achieving low noise media by scaling to smaller grain size, however, is limited by thermal instabilities, which may render today's commonly used Co-alloy-based recording media unsuitable for archival data storage at extremely high area densities.[1,3] Recently, there has been much attention placed on the chemical synthesis of self-assembled, monodispersed, and chemically ordered $L1_0$ (tetragonal phase) FePt nanoparticles for future ultrahigh-density magnetic storage.[4–8] In fact, recent advances in magnetic recording technology have indicated that, if self-assembled in a tightly packed, exchange-decoupled array with controlled magnetic easy axis direction, these FePt nanoparticles could support high-density magnetization reversal transitions and would be a candidate for future ultrahigh-density data storage media[8–10] with potentially one bit per particle corresponding to storage densities of 20 Tbit/in.^{2} The tetragonal phase of an FePt system is of particular interest because of the high magnetocrystalline anisotropy [$K_U \sim (6.6-10) \times 10^7$ erg/cm^3] that should allow the use of smaller particles, but yet avoid thermal instabilities that give rise to superparamagnetic (SPM) behavior.[3,11] Since the medium magnetic stability is controlled by the ratio of the magnetic anisotropy energy, K_UV, to the energy of thermal fluctuations, k_BT, where K_U is the recording layer magnetic anisotropy energy density and V is the thermal activation volume, which corresponds approximately to the volume of a single magnetic grain, and the k_BT are Boltzmann's constant and the temperature, respectively. The ratio K_UV/k_BT is kept at a value of 50–70 to ensure 10–15 years data stability.[2,3,12] Although the structural and magnetic properties of FePt have been intensively studied as a function of composition,[13] there are a few number of works that have studied these nanoparticles when the FePt composition is set in $Fe_{55}Pt_{45}$, which is reported as expected to present the highest magnetic properties in the ordered $L1_0$ phase.[8,13] For bulk alloys, these structural and magnetic properties are known. However, due to the difficulty of stabilizing $Fe_{55}Pt_{45}$ phase as nanoparticle material, the small size and the larger surface area of the particles affect these properties and, consequently, the ordering process during the $L1_0$ phase formation could be also affected. Recently, we have modified the synthetic procedure reported by Sun *et al.*[6] to prepare monodisperse and self-assembled FePt ferromagnetic nanocrystals (4.0±0.2 nm) with compositions ranging

[a]Author to whom correspondence should be addressed. Present address: Instituto de Química de São Carlos, USP, CP 780, 13560-970 São Carlos, SP, Brazil; electronic mail: lvaranda@iqsc.usp.br; Tel.: +55 16 3301 6651; Fax: +55 16 3301 6692.

from $Fe_{48}Pt_{52}$ to $Fe_{62}Pt_{38}$. This modification in the synthetic polyol route improved the nanoparticle composition control by changing the volatile and toxic $Fe(CO)_5$ (iron pentacarbonyl) by $Fe(acac)_3$ (iron acetylacetonate) isopropanolic hot solution.[8] Although Takahashi *et al.* have recently reported the FePt nanoparticles preparation using a methodology described as a modified polyol process and $Fe(acac)_3$ as an iron source,[14] the synthetic route used in this work is slightly different. According to the reported results by Takahashi *et al.*, the FePt nanoparticle morphology was very heterogeneous, presenting strong surface irregularity and faceted particles. In our previous studies, the same behavior was observed when $Fe(acac)_3$ was used as solid salt directly in the reaction mixture, probably due to slow salt solubility in the hot organic solvent (~100 °C). On the other hand, we recently reported[8] highly spherical homogeneous particle morphology of monodisperse 4 nm $Fe_{55}Pt_{45}$ with chemical composition control when solid $Fe(acac)_3$ salt was replaced to solubilized salt in a hot isopropanolic solution due to enhance Fe(III) distribution in the reaction mixture. Since the structural and magnetic properties of the FePt nanoparticles are strongly dependent on the nanoparticle composition, our improvement in the composition control allowed stabilizing the $Fe_{55}Pt_{45}$ phase, which is a strong candidate for ultrahigh-density storage devices.

As shown in a previous article,[8] the high coercivity value of about 12 kOe was observed in a self-assembled $Fe_{55}Pt_{45}$ nanoparticle in a cubic array. In this work, we report the temperature (blocking temperature) and the uniaxial magnetocrystalline anisotropy constant dependence of coercive field as a function of the annealing temperature for a chemically synthesized $L1_0$-$Fe_{55}Pt_{45}$ nanoparticle array. We also show the magnetic behavior of the assembled sample at low and room temperatures in order to evaluate the magnetic interparticle coupling and ferromagnetic nanocrystals transformation with increased annealing temperature.

II. EXPERIMENTAL

A synthetic procedure based on the modified polyol process to produce Fe_xPt_{1-x} nanoparticles was reported earlier.[8] Monodisperse $Fe_{55}Pt_{45}$ nanoparticles were synthesized as follows: in a three-neck round-bottom flask, a mixture of $Pt(acac)_2$ (0.4 mmol) and 1,2-hexadecanediol (1.2 mmol) in octylether (20 mL) was heated at 100 °C. Then, oleic acid (0.4 mmol), oleylamine (0.4 mmol), and isopropanolic hot-solution preheated at 70 °C of $Fe(acac)_3$ (0.49 mmol in Fe) were added to the mixture via syringe. Temperature was increased and the system maintained under reflux (298 °C) for 30 min. Particles were separated by ethanol addition, isolated by centrifuging (three times), and dried in a vacuum oven at room temperature. Self-assembled nanostructures in cubic arrays were obtained redispersing the nanoparticles in a 50/50 mixture of hexane and octane containing 0.1 mL of 50/50 mixture of short-chain capping groups such as hexanoic acid and hexylamine.[8,15] As-deposited thin films were then transferred into a tube furnace (Thermolyne 1300) and annealed for 30 min with flowing nitrogen containing 5% hydrogen at temperatures ranging from 400 to 600 °C.

Morphology, particle size, and size distribution were investigated by transmission electron microscopy (TEM) using a Philips CM200 microscope operating at 200 kV. For TEM analysis, the as-prepared self-assembled nanoparticle suspension was dropped onto the carbon-coated copper grid. Then, samples were transferred to the furnace and annealed at temperatures ranging from 400 to 600 °C for 30 min in a N_2:H_2 mixed atmosphere. Average particle size diameter (d) and their standard deviation (σ) were statistically determined in order to obtain the degree of polydispersity (δ) of the systems. The nanoparticle composition was determined by inductively coupled plasma-atomic emissions (ICP) performed in a Plasma 40 Perkin Elmer spectrometer, and nanoparticle structure characterization was carried out by x-ray powder diffraction (XRD) on a Rigaku RINT2000 diffractometer using Cu $K\alpha$ radiation. Magnetic studies were carried out using a conventional SQUID magnetometer in temperatures ranging from 5 to 400 K. Measurements were done on thick nanoparticle assemblies (>100 nm) on a silica micro slide (0.5×0.5 cm) and loaded perpendicular and parallel to the magnetic field.

III. RESULTS AND DISCUSSION

Monodisperse FePt nanoparticles of 4.0 ± 0.2 nm with polydispersity degree lower than 5%,[16] both determined by statistical analysis using transmission electron microscopy (TEM), were obtained and self-assembled in a cubic nanostructure array as presented in Fig. 1. The results in Fig. 1 correspond to the annealed sample at 550 °C for 30 min and show the maintenance of long-range order of the particles and that coalescence and/or sintering processes were absent. ICP analysis showed that composition of the resulting FePt nanoparticles is $Fe_{55}Pt_{45}$. In addition, energy-dispersive x-ray analysis (EDS) was performed during the TEM analysis on many individual nanoparticles or in a group of a few nanoparticles. The results of both techniques, EDS and ICP, are in good agreement, indicating high compositional homogeneity. TEM image of the cubic array [Fig. 1(b)] has a surface area of about 55×40 nm^2 and comprises about 100 monolayered particles. Thus, the corresponding particle density per surface unit area is ~26 T particles/$in.^2$ In a desirable future single particle per bit patterned recording scheme, this could lead to respective areal bit densities of 26 Tbit/$in.^2$. Additionally, the inset in Fig. 1(b) shows the high-resolution TEM (HRTEM), indicating a lattice spacing of 2.20 Å, characteristic of (111) planes of $L1_0$-$Fe_{55}Pt_{45}$ phase. The texture presented in the HRTEM implies high structural homogeneity of the face-centered tetragonal phase ($L1_0$) and indicates the formation of nanocrystals after annealing, in agreement with the previous results of XRD, structural, and average crystallite size analysis, which indicate nanocrystal formation in the sample annealed at 550 °C.[8]

The influences of the annealing temperature on the chemical ordering, magnetic properties, and interparticle magnetic coupling were studied by measuring the temperature-dependent magnetic properties in the temperatures ranging from 5 to 400 K. Figure 2 shows a series of hysteresis curves obtained for as-synthesized $Fe_{55}Pt_{45}$ nano-

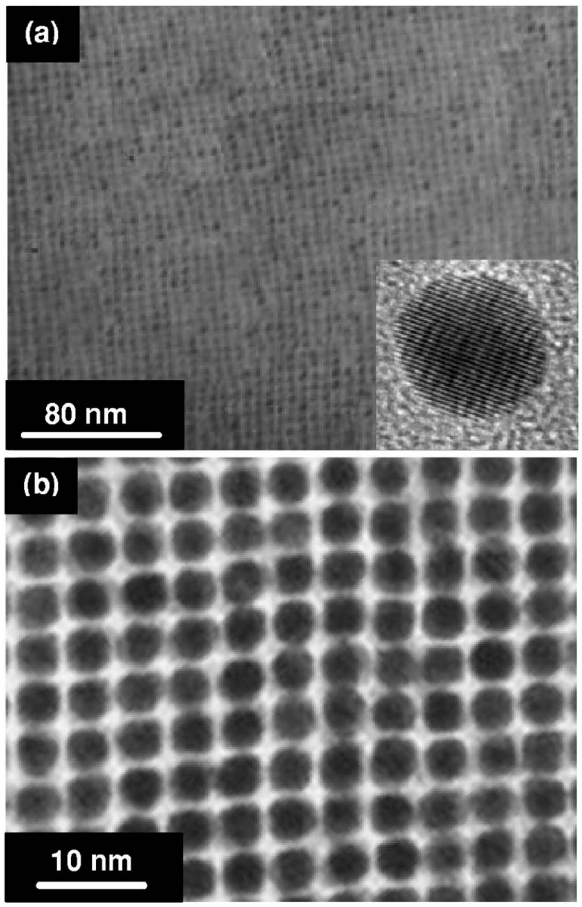

FIG. 1. Representative TEM images of a cubic array 2D assembly of chemically synthesized $Fe_{55}Pt_{45}$ nanoparticles with 4 nm diameter after annealing at 550 °C for 30 min: (a) low and (b) high magnification. The inset correspond to the HRTEM showing the texture of an individual nanoparticle along the (111) plane.

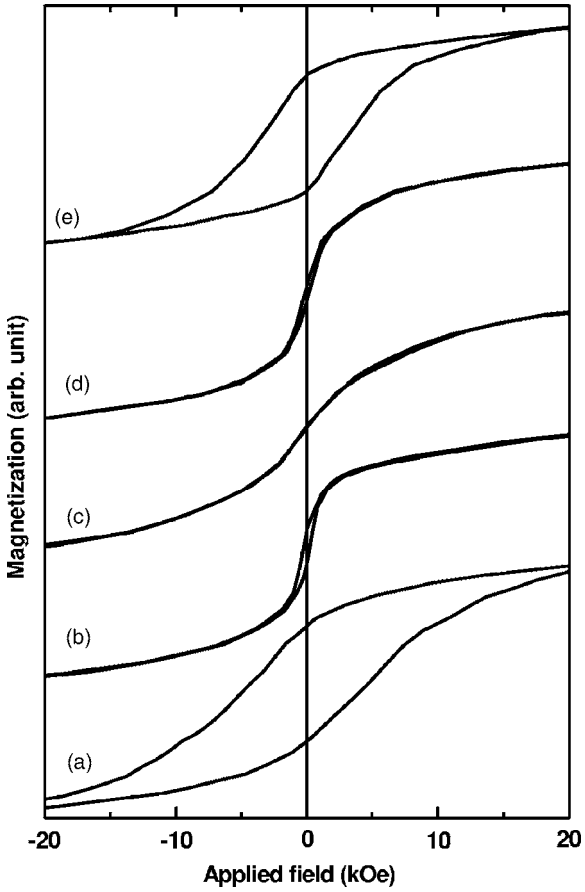

FIG. 2. Hysteresis loops of the as-synthesized $Fe_{55}Pt_{45}$ nanoparticles assembly at (a) 5 K, (b) 15 K, (c) 50 K, and measured at room temperature after annealing at (d) 400 °C and (e) 500 °C.

particles assembly at low-temperature [Figs. 2(a)–2(c)] and at room-temperature hysteresis loops after sample annealing at 400 °C [Fig. 2(d)] and 500 °C [Fig. 2(e)]. Hysteresis loop of the as-prepared nanoparticles assembly showed that they are superparamagnetic (SPM) at room temperature. However, at low temperature, the assembled nanoparticles show ferromagnetic behavior, as indicated by Fig. 2(a), with a coercivity value (H_C) around 4.3 kOe at 5 K. The coercivity drops sharply as temperature is raised from 5 to 15 K, the latter presenting H_C=250 Oe suggesting that these nanoparticles are thermally unstable. These results are consistent with the low magnetocrystalline anisotropy of the fcc phase presented by as-synthesized nanoparticles and with the SPM oxide shell, in agreement with the literature.[8,13,17] At 50 K, the assembly shows SPM behavior similar to that observed for these nanoparticles at room temperature. Low-temperature hysteresis behavior presented in Fig. 2 also suggests that the blocking temperature of the $Fe_{55}Pt_{45}$ nanoparticles is closed around 20 K. The coercivity values increase dramatically with annealing temperature showing the transition from superparamagnetic to ferromagnetic behavior. The hysteresis loop of the sample annealed at 400 °C appears nearly SPM at room temperature, presenting H_C=150 Oe and suggesting a minority fraction of the particles having sufficient anisotropy to be ferromagnetically ordered at room temperature. When the annealing temperature is increased to 500 °C, the ferromagnetic fraction of the $Fe_{55}Pt_{45}$ nanoparticles increases and the H_C assume a value of 3.6 kOe, but the curve shows an inflection in the magnetizations near H =0, indicating that some low H_C particles are present. Annealing at 550 °C results in a room-temperature H_C value of 12.1 kOe with a loop shape characteristic of an isotropic distribution of high anisotropy particles (Fig. 3). Annealing converts the internal particle structure from fcc to $L1_0$ phase

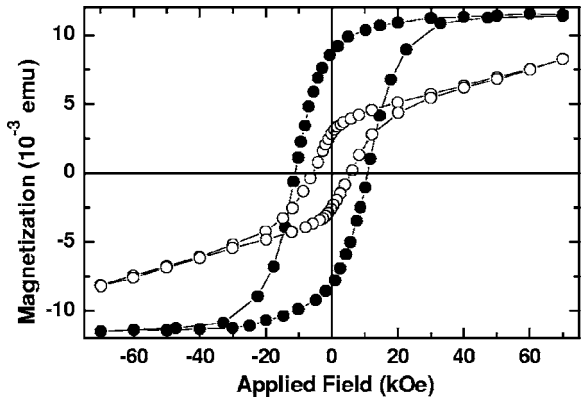

FIG. 3. In-plane (open circles) and out-of-plane (filled circles) room-temperature hysteresis loops of $Fe_{55}Pt_{45}$ nanoparticle assemblies annealed at 550 °C for 30 in.

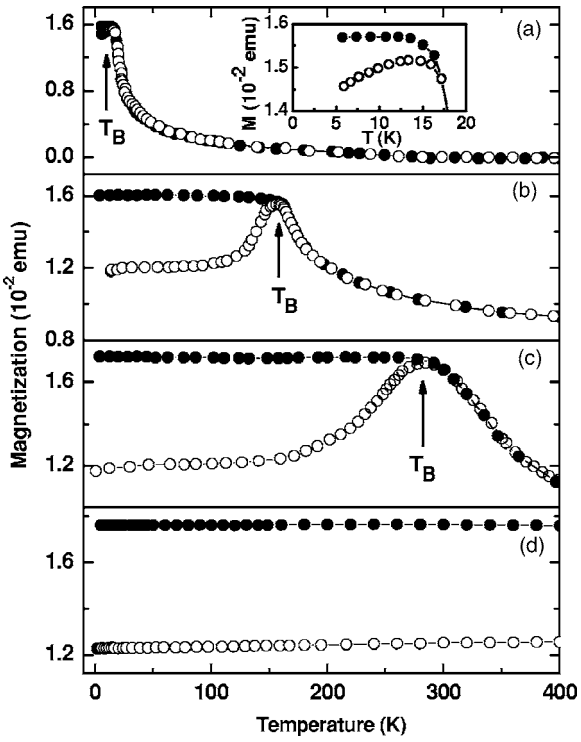

FIG. 4. Magnetization vs temperature measured at 100 Oe in the zero-field-cooled (open circles) and field-cooled (filled circles) states for $Fe_{55}Pt_{45}$ nanoparticle assembly (a) as-synthesized and annealed at (b) 400 °C, (c) 500 °C, and (d) 550 °C. Inset shows the blocking temperature position for as-synthesized nanoparticles.

(fct) and transforms the SPM nanoparticles into ferromagnetic nanocrystal assemblies with larger coercivity at room temperature. The significant difference between in-plane (H_C=5.8 kOe) and out-of-plane (H_C=12.1 kOe) coercivity values and the hysteresis behavior presented in Fig. 3 indicates a nonrandom orientation or, at least, a partial orientation of the easy axes of the individual $L1_0$-$Fe_{55}Pt_{45}$ nanocrystals. Although the obtained H_C value is larger than those reported for different compositions of FePt nanoparticles[6,8,13] confirming the highest expected coercivity value for the $L1_0$-$Fe_{55}Pt_{45}$ phase, the obtained coercivity values are much smaller than those expected of the FePt bulk. Thus, this result suggests that the same magnetic disorder still remains and interparticle interaction effects can be present. In addition, the remanence ratio is $S=M_R/M_S \cong 0.76$, compatible with an average c-axis orientation of 40.5° ($\cos 40.5° = 0.76$), which is expected for (111) textured films.[3] In Fig. 3, we can also observe the difference in the saturation magnetization (M_S) behavior when the sample was measured with in-plane and out-of-plane applied field. Out-of-plane measurement showed that the sample was found to be magnetically saturated around 35 kOe; when the field was applied longitudinal to the film surface (in-plane), the magnetic saturation could not be observed in the used field range. This result suggests strong interparticle coupling in this direction, in agreement with the partial orientation of the easy magnetic axis of the individual ferromagnetic nanocrystals and with the calculated c-axis orientation. In the temperature dependence of magnetization (Fig. 4) measurements, both the zero-field-cooling (M_{ZFC}) and field-cooling (M_{FC}) processes were carried out at field H=100 Oe. The M_{ZFC} curve for as-synthesized nanoparticles shows a sharp peak with a maximum at low temperature as indicated in Fig. 4(a), characteristic of a narrow particle size distribution or interparticle noninteracting systems. The blocking temperature estimated from curves in Fig. 4(a) is T_B=17 K, which agrees with the low-temperatures hysteresis results presented in Fig. 2, and the coincident point of both the M_{ZFC} and M_{FC} curves suggests a reversible process, as expected for an fcc phase in a SPM state. The sample annealed at 400 °C [Fig. 4(b)] showed a peak with a maximum at 160 K in the M_{ZFC} curve, which corresponds to the blocking temperature. The shape of the M_{ZFC} curve can be associated with hard magnetic systems, in which the thermal irreversibility of magnetization is directly correlated with the magnetocrystalline anisotropy and, therefore, to the coercivity of the materials. The low field M_{ZFC} curve shows a sharp decrease below T_B in the temperature region where $H_C(T)$ is linear and becomes almost constant below ~100 K. These results indicate that the drop in the magnetization below T_B is related to the magnetic hysteresis behavior. Since the FePt nanoparticles present a high coercive field, as shown by low-temperature magnetic hysteresis loops, at low temperature the H_C values are always larger than an applied field of 100 Oe, and the magnetization remains constant after the observed decreasing below T_B. The broadening peak shown in the M_{ZFC} for a sample annealed at 400 °C was assigned to magnetic domains formation due to the evolution from fcc to $L1_0$ phase transformation as indicated by room-temperature hysteresis loops [Fig. 2(d)]. Moreover, according to the T_B value of 160 K, the nanoparticles are found to be SPM; the H_C of 150 Oe presented by these samples can be explained because of the broad coercive distribution as shown by the M_{ZFC} curve. At 400 K, the magnetization value is $\sim 1.0 \times 10^{-2}$ emu, indicating a minority fraction of the particles having sufficient anisotropy to be ferromagnetically ordered at room temperature. In the field-cooled measurement, the sample is cooled in a magnetic field through the ordering temperature and therefore the resultant magnetization is determined by the net direction of the spins depending on the strength of the applied field. The same magnetic field applied after cooling the sample in zero magnetic field may not be sufficient to rotate the spins that are locked in random directions due to the high anisotropy. Therefore, the resultant magnetization will be lower than that obtained during the field-cooled process, and both M_{ZFC} and M_{FC} also remain constant below T_B. The sample annealed at 500 °C [Fig. 4(c)] presented the same behavior and the T_B=284 K, in agreement with the $M \times H$ curve, which showed ferromagnetic behavior at room temperature. The broadening peak in the M_{ZFC} curve is larger than the sample annealed at 400 °C, probably due to ferromagnetic fraction particles increasing. As shown by the room-temperature hysteresis loop for the sample annealed at 550 °C, the $Fe_{55}Pt_{45}$ nanoparticle assembly is ferromagnetic and presents larger coercivity, in agreement with the results of the M_{ZFC} and M_{FC} curves [Fig. 4(d)], which are found to be constant at a temperature up to 400 K.

The temperature dependence of H_C for different annealing temperatures is shown in Fig. 5. Each sample shows a

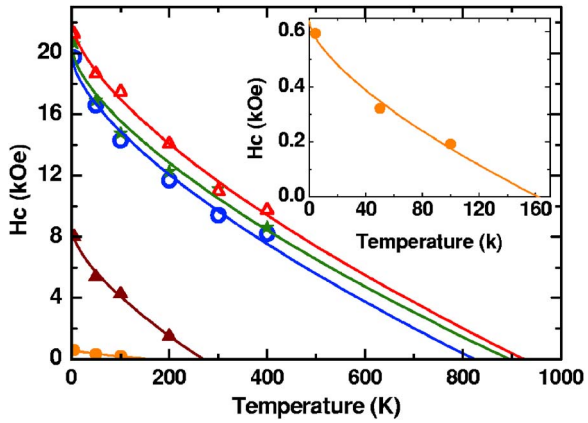

FIG. 5. (Color online) Temperature-dependent H_C of $Fe_{55}Pt_{45}$ nanoparticle assembly annealed at 400 °C (orange ●), 500 °C (wine ▲), 550 °C (blue ○), 580 °C (green ★), and 600 °C (red △). The symbols are the experimental data and the lines correspond to the fits. Inset shows in detail the curve of the annealed sample at 400 °C.

monotonic increase in H_C with decreasing temperature. The H_C behavior can be quantitatively understood by relating the measured coercivity to the low-temperature coercivity, H_0, and the stability factor (K_UV/k_BT),[12,18]

$$H_c = H_0\left\{1 - \left[\frac{k_BT}{K_UV}\ln\left(\frac{t_Pf_0}{\ln 2}\right)\right]^{2/3}\right\}, \quad (1)$$

where K_U, V, k_B, and T were previously defined, t_P is the time of magnetic field applied (~5 s), and f_0 is the thermal attempt frequency ($\sim 10^9$ Hz). The fits of the data in Fig. 5 to the Eq. (1), where the K_UV is assumed to be constant with temperature, yield H_0 values of 0.4, 8.5, 19.7, 20.3, and 21.98 kOe, respectively, for samples annealed at 400, 500, 550, 580, and 600 °C, extrapolating the fits to $T=0$. Assuming that V is determined by the individual grain volume, K_U can be estimated showing values of 1.4×10^7, 2.3×10^7, 7.2×10^7, 7.8×10^7, and 8.0×10^7 erg/cm^3 for annealing temperatures at 400, 500, 550, 580, and 600 °C, respectively. The K_U values of 7.2×10^7 erg/cm^3 of 550 °C annealed sample agree with that expected for fully ordered FePt $[(6.6-10)\times10^7$ erg/cm$^3]$. The blocking temperature can also be estimated by extrapolation of the fit curves at $H_C=0$. The obtained values of 160 and 285 K for FePt samples annealed at 400 and 500 °C, respectively, are in good agreement with the zero-field-cooled measurements of the magnetization, which shows peaks near these temperatures (Fig. 4). The room-temperature stability parameter for the $Fe_{55}Pt_{45}$ nanoparticle assembled annealed at 550 °C is $K_UV/k_BT=67$, which indicates that the magnetization should be stable for more than ten years and makes this material suitable for ultrahigh-density magnetic recording application.

IV. CONCLUSIONS

We have investigated the effect of annealing temperature on the magnetic properties and on uniaxial magnetocrystalline anisotropy of $L1_0$-$Fe_{55}Pt_{45}$ nanoparticles assembly synthesized by a modified polyol process, which promoted the improved morphology and composition control. As-synthesized, the nanoparticles are SPM, and annealing at 550 °C converts the nanoparticles in a ferromagnetic nanocrystals with larger coercivity ($H_C>1$ T). An increase in the ferromagnetically ordered fraction of the nanoparticles with the annealing temperature increase was observed by magnetic measurements, and the remanence ratio, $S=M_R/M_S \cong 0.76$, which is compatible with an average c-axis orientation of 40.5°, suggests a (111) textured films. We have also observed a monotonic increase of the blocking temperature T_B, the uniaxial magnetocrystalline anisotropy constant K_U, and the coercivity H_C with increasing annealing temperature. Magnetic parameters indicate an enhancement in the magnetic properties due to the improved $Fe_{55}Pt_{45}$ phase stabilizing and composition control. Additionally, a room-temperature stability parameter of 67 indicates that the magnetization should be stable for more than ten years, making this material suitable for ultrahigh-density magnetic recording application.

ACKNOWLEDGMENTS

This work was financially supported by the Brazilian agency FAPESP, award Nos. 04/06762-0 and 04/02407-1.

[1]D. Weller, S. Sun, C. B. Murray, L. Folks, and A. Moser, IEEE Trans. Magn. **37**, 2185 (2001).
[2]E. Chunsheng, D. Smith, J. Wolfe, D. Weller, S. Khizroev, and D. Litvinov, J. Appl. Phys. **98**, 024505 (2005).
[3]D. Weller, A. Moser, L. Folks, M. E. Best, W. Le, M. F. Toney, M. Schweickert, J. R. Thiele, and M. F. Doerner, IEEE Trans. Magn. **36**, 10 (2000).
[4]S. Kang, J. W. Harrell, and D. E. Nikles, Nano Lett. **2**, 1033 (2002).
[5]T. J. Klemmer, N. Shukla, C. Liu, X. W. Wu, E. B. Svedberg, O. Mryasov, R. W. Chantrell, and D. Weller, Appl. Phys. Lett. **81**, 2220 (2002).
[6]S. Sun, C. B. Murray, D. Weller, L. Folks, and A. Moser, Science **287**, 1989 (2000).
[7]E. V. Shevchenko, D. V. Talapin, H. Schnablegger, A. Kornowski, O. Festin, P. Svedlindh, M. Haase, and H. Weller, J. Am. Chem. Soc. **125**, 9090 (2003).
[8]L. C. Varanda and M. Jafelicci, Jr., J. Am. Chem. Soc. **128**, 11062 (2006).
[9]S. Anders, M. F. Toney, T. Thomson, J. U. Thiele, B. D. Terris, S. H. Sun, and C. B. Murray, J. Appl. Phys. **93**, 7343 (2003).
[10]S. H. Sun, S. Anders, T. Thomson, J. E. E. Baglin, M. F. Toney, H. F. Hamann, C. B. Murray, and B. D. Terris, J. Phys. Chem. B **107**, 5419 (2003).
[11]S. H. Charap, P. L. Lu, and Y. J. He, IEEE Trans. Magn. **33**, 978 (1997).
[12]D. Weller and A. Moser, IEEE Trans. Magn. **35**, 4423 (1999).
[13]S. Sun, E. E. Fullerton, D. Weller, and C. B. Murray, IEEE Trans. Magn. **37**, 1239 (2001).
[14]B. Jeyadevan, K. Urakawa, A. Hobo, N. Chinnasamy, K. Shinoda, K. Tohji, D. D. J. Djayaprawira, M. Tsunoda, and M. Takahashi, Jpn. J. Appl. Phys., Part 2 **42**, L350 (2003).
[15]M. Chen and D. E. Nikles, Nano Lett. **2**, 211 (2002).
[16]R. J. Hunter, *Foundations of Colloid Science* (Clarendon, Oxford, UK, 1989), pp. 104–130.
[17]T. Thomson, M. F. Toney, S. Raoux, S. L. Lee, S. Sun, C. B. Murray, and B. D. Terris, J. Appl. Phys. **96**, 1197 (2004).
[18]M. P. Sharrock, IEEE Trans. Magn. **35**, 4414 (1999).